MAGNETIC MATERIALS

Reconfigurable ferromagnetic liquid droplets

Xubo Liu[1,2], Noah Kent[2,3], Alejandro Ceballos[4], Robert Streubel[2], Yufeng Jiang[2,5], Yu Chai[2,4,6], Paul Y. Kim[2], Joe Forth[2], Frances Hellman[2,7], Shaowei Shi[1], Dong Wang[1,8], Brett A. Helms[2,6], Paul D. Ashby[2,6], Peter Fischer[2,3], Thomas P. Russell[1,9,10]*

Solid ferromagnetic materials are rigid in shape and cannot be reconfigured. Ferrofluids, although reconfigurable, are paramagnetic at room temperature and lose their magnetization when the applied magnetic field is removed. Here, we show a reversible paramagnetic-to-ferromagnetic transformation of ferrofluid droplets by the jamming of a monolayer of magnetic nanoparticles assembled at the water-oil interface. These ferromagnetic liquid droplets exhibit a finite coercivity and remanent magnetization. They can be easily reconfigured into different shapes while preserving the magnetic properties of solid ferromagnets with classic north-south dipole interactions. Their translational and rotational motions can be actuated remotely and precisely by an external magnetic field, inspiring studies on active matter, energy-dissipative assemblies, and programmable liquid constructs.

Ferromagnetic materials are generally solids with a fixed shape. Reconfigurable magnetic materials are known, such as ferrofluids [dispersions of magnetic nanoparticles (MNPs) in carrier fluids], but they are paramagnetic and lose magnetization once the external magnetic field is removed (*1*, *2*). Ferrofluids exhibit interesting properties and have found use, for example, as magnetic seals, but their inability to retain magnetization limits their broader application. The transformation of a ferrofluid into a ferromagnetic material can be realized by lowering the temperature or increasing the viscosity, at which Brownian motion of the MNPs is suppressed. Here, we show a simple means to effect this transformation by the in situ formation and interfacial jamming of MNP-surfactants.

We immersed an aqueous dispersion of carboxylated 22-nm-diameter MNPs (Fe_3O_4-CO_2H) in a solution of amine-modified polyhedral oligomeric silsesquioxane (POSS-NH_2) in toluene. The POSS-NH_2, itself a surfactant, assembles at the interface and electrostatically interacts with the MNPs, anchoring a well-defined number of POSS-NH_2 to the MNPs, converting the MNPs into MNP-surfactants. When the droplet shape changes, the interfacial area increases, and additional MNP-surfactants form and assemble at the interface. The droplet proceeds to reshape itself to minimize the interfacial area and, thereby, the free energy of the system, but the MNP-surfactants are compressed and jam, locking in the deformed shape (*3*, *4*) while remaining magnetized even without an external field.

Magnetic hysteresis loops of Fe_3O_4-CO_2H ferrofluid droplets (Fig. 1A), measured by a vibrating sample magnetometer, show a saturation magnetization (M_s) that depends on the total number of MNPs in the droplets, as well as a vanishing coercive field (H_c) and remanent magnetization (M_r). By adding POSS-NH_2 ligands to the toluene, MNP-surfactants form at the interface. Increasing the concentration of the MNPs in the droplet or decreasing pH increases the coverage of the interface by MNP-surfactants, reducing the interfacial tension (fig. S1, A and B). With sufficient surface coverage, the MNP-surfactants jam, and the ferrofluid droplet transforms into a ferromagnetic liquid droplet. The magnetic hysteresis loops of identical ferrofluid droplets with and without the jammed interfacial assemblies of MNP-surfactants are shown in Fig. 1A. For both, M_s is the same because the total number of MNPs is identical, but M_r ~1.89×10^{-8} A m^2 and H_c ~7.2 kA m^{-1} for the ferromagnetic liquid droplet, demonstrating their ferromagnetic character. The jammed, interfacial assemblies of the MNP-surfactants are disordered and have a mechanical rigidity that suppresses thermal fluctuations characteristic of isolated MNPs. The jammed MNPs no longer freely rotate. The spatial separation between adjacent MNP-surfactants is <5 nm, which, combined with the orientation of the dipole magnetization in the MNPs, enhances the thermal stability of the magnetization and transforms the droplet surface into a ferromagnetic layer, similar to a fixed assembly of MNPs (*5*, *6*). When the field is removed, the moment of the ferromagnetic liquid droplet remains until the droplet is exposed to a field exceeding the switching field, whereupon the droplet is remagnetized. Reshaping the droplet by other external fields or reducing the binding energy of the MNP-surfactants will also unjam the MNP-surfactants (M_r and H_c vanish), providing further routes to control the magnetization. This ability to manipulate the magnetization further distinguishes ferromagnetic liquid droplets from ferrofluids and common ferromagnetic materials.

If the MNP-surfactant assembly is not jammed, no hysteresis is observed (Fig. 1B). To produce droplets with an unjammed assembly, the surface coverage of the droplets with the MNP-surfactants is varied from ~7 to ~20% (fig. S1C) by changing the concentrations of the MNPs and POSS-NH_2 and the pH. In Fig. 1B, variations in M_s arise from differences in the total number of MNPs in each droplet. With full MNP-surfactant coverage—for example, single droplets of [Fe_3O_4-CO_2H MNPs] = 0.5 g L^{-1} at pH 4.5 in toluene containing [POSS-NH_2] = 1.0 g L^{-1}—the interfacial assembly jams, and a typical ferromagnetic hysteresis loop is seen (Fig. 1C). Hysteresis loops were measured for single droplets with different volumes, and the same droplets sonicated into numerous smaller droplets. This preserves the total volume (summed over all droplets) of the MNP dispersions but increases the surface-to-volume ratio (S/V) by two orders of magnitude (fig. S2D). M_s and M_r scale linearly with the total volume (total number of MNPs), whereas H_c remains constant (Fig. 1C). For a given total volume, M_r is independent of S/V with largely varying droplet sizes. The mean separation distance between the dispersed MNPs is ~350 nm, too large for dipolar coupling. For comparison, discs that are 100 nm in diameter and 10 nm thick and have much larger saturation magnetizations are completely uncorrelated when the separation distance is >60 nm (*7*). The MNPs dispersed in the droplet freely diffuse, yet a strong coupling and correlation of the dispersed MNPs to those jammed at the interface is evident, and the liquid droplets behave like solid magnets. Furthermore, the ratio of M_r/M_s for the ferromagnetic liquid droplets is 0.25, independent of droplet volume, which is the same as that for frozen ferrofluids at 4.5 K and fixed assemblies of Fe_3O_4 MNPs (*8*–*10*). Consequently, ferromagnetic liquid droplets have a similar energy barrier to overcome during magnetization reversal

[1]Beijing Advanced Innovation Center for Soft Matter Science and Engineering, Beijing University of Chemical Technology, Beijing 100029, China. [2]Materials Sciences Division, Lawrence Berkeley National Laboratory, Berkeley, CA 94720, USA. [3]Physics Department, University of California, Santa Cruz, Santa Cruz, CA 95064, USA. [4]Department of Materials Science and Engineering, University of California, Berkeley, Berkeley, CA 94720, USA. [5]Department of Applied Science and Technology, University of California, Berkeley, Berkeley, CA 94720, USA. [6]The Molecular Foundry, Lawrence Berkeley National Laboratory, Berkeley, CA 94720, USA. [7]Physics Department, University of California, Berkeley, Berkeley, CA 94720, USA. [8]State Key Laboratory of Organic–Inorganic Composites, Beijing University of Chemical Technology, Beijing 100029, China. [9]Polymer Science and Engineering Department, University of Massachusetts, Amherst, MA 01003, USA. [10]WPI–Advanced Institute for Materials Research (WPI-AIMR), Tohoku University, Sendai 980-8577, Japan.
*Corresponding author. Email: tom.p.russell@gmail.com

as their frozen or solid counterparts. Therefore, ferromagnetic liquid droplets have the magnetic properties of a solid.

All-liquid printing (*11*–*13*) and microfluidics (*14*) were used to produce ferromagnetic liquid cylinders with a 2:1 aspect ratio (fig. S3). A nonmagnetized ferromagnetic liquid cylinder was transferred to a toluene/CCl_4 density gradient in which the cylinder descended until buoyant (fig. S4, A and B). The axis of the cylinder and an insulated solenoid were aligned (Fig. 2A), and a magnetic field of 1 to ~2 kA m^{-1} (Fig. 2B) applied to the solenoid pulled the ferromagnetic liquid cylinder into the solenoid. The cylinder reached the solenoid in 30 s at a speed of ~1.1 × 10^{-4} m s^{-1} and stopped after fully entering the solenoid because of the absence of drag forces.

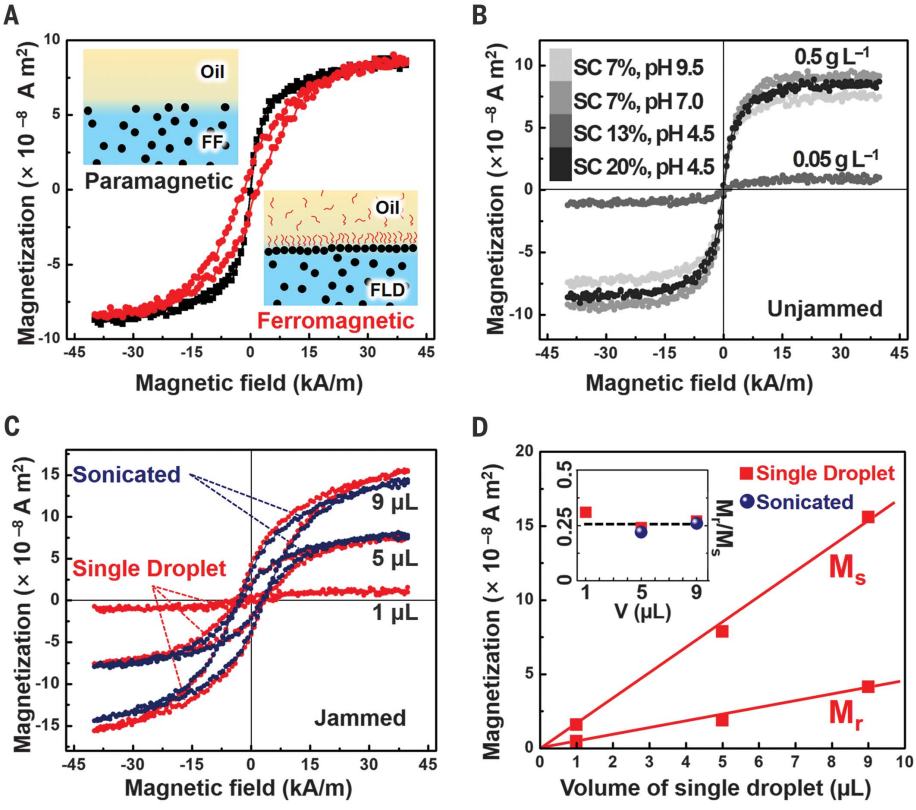

Fig. 1. Tunable transformation of a paramagnetic FF into an FLD by the interfacial jamming of MNP-surfactants. (**A**) Magnetic hysteresis loops of droplets with (red line) and without (black line) an interfacial layer of jammed MNP-surfactants measured with a vibrating sample magnetometer. Two schematics of aqueous FF and FLD, containing Fe_3O_4-CO_2H MNPs (0.5 g L^{-1}) at pH 4.5, immersed in toluene without and with POSS-NH_2 ligands (1.0 g L^{-1}). (**B**) Hysteresis loops of individual 5-µL aqueous droplets, with 0.5 g L^{-1} and 0.05 g L^{-1} of Fe_3O_4-CO_2H MNPs at different pH, immersed in 0.01 g L^{-1} ligand solution. Surface coverage (SC) of droplets is ~7 to ~20% where MNPS assemblies are not jammed. (**C**) Hysteresis loops of single, jammed aqueous droplets with 0.5 g L^{-1} of MNPs at pH 4.5 immersed in a 1.0 g L^{-1} solution of POSS-NH_2 in toluene and hysteresis loops of the same system after being sonicated (figs. S1 and S2). (**D**) M_r and M_s of the droplets as a function of droplet volume. In the inset, the remanence ratio M_r/M_s as a function of initial droplet volume (single droplet or droplet sonicated into multiple smaller droplets) remains constant at ~0.25. FF, ferrofluid; FLD, ferromagnetic liquid droplet.

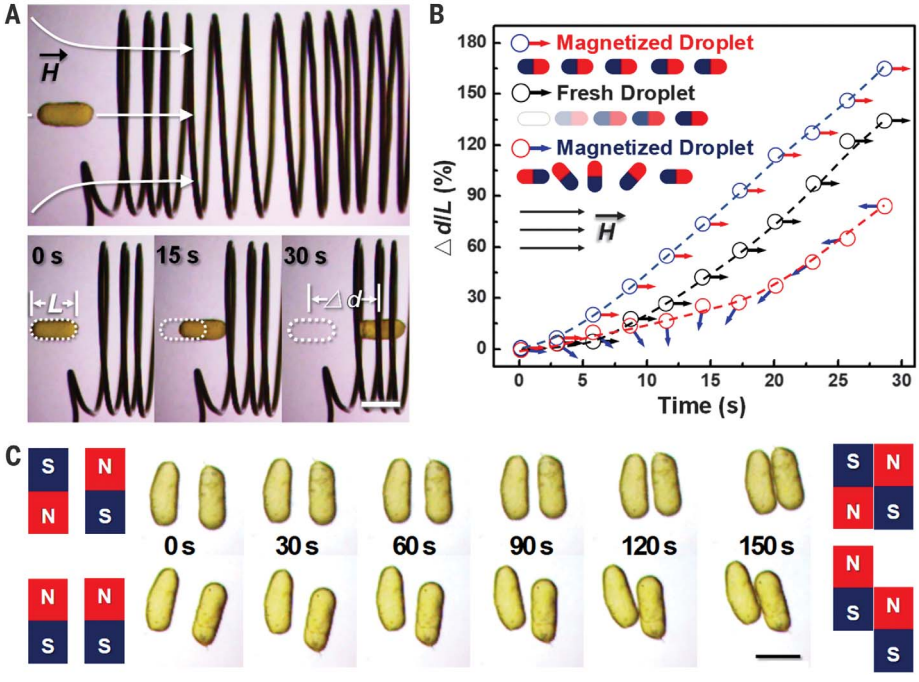

Fig. 2. Manipulating FLDs with magnetic dipole interactions. (**A**) A magnetized liquid cylinder is attracted by a magnetic field gradient, generated by the aluminum solenoid. (**B**) Displacement as a function of time for fresh, nonmagnetized liquid cylinder (black arrow), magnetized liquid cylinder with north pole facing the coil (red arrow), and magnetized liquid bar with south pole facing the coil (blue arrow). The ultimate velocity is determined by the field gradient and magnetic moment. The arrows indicate the orientation of the cylinder relative to the initial orientation. (**C**) Dipole interactions, N–S attraction, N–N and S–S repulsion, between two magnetized liquid cylinders. Scale bars, 2 mm.

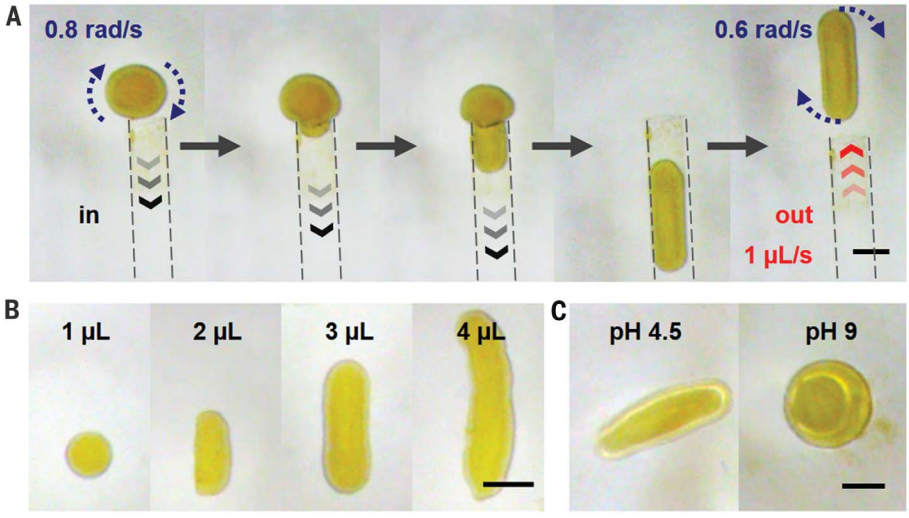

Fig. 3. Top view of deforming an FLD. (**A**) Reshaping spherical droplet into the cylinder by mechanically molding it with the glass capillary channel. (**B**) Droplets of different aspect ratios can be formed by using droplets with different volumes. (**C**) Reconfiguration of interfacial jamming and unjamming of MNP-surfactants by tuning the pH (for example, 4.5 and 9, respectively) of aqueous solution in the FLD cylinder. Scale bars, 1 mm.

The displacement, Δd (in units of the droplet length, L), allows comparison of different ferromagnetic liquid cylinders because the drag force varies linearly with length, which for a fixed cylinder radius corresponds to the volume and M_s. Figure 2A shows the location and direction of the magnetic moment of the ferromagnetic liquid cylinder. The cylinder, magnetized only by the solenoid, moved inside the solenoid (movie S1). This ferromagnetic liquid cylinder (now magnetized) was repositioned outside the solenoid, preserving the south-north (S–N) pole orientation. With the same solenoid magnetic field strength (1 to ~2 kA m^{-1}), the cylinder now accelerates to the solenoid (Fig. 2B and movie S2). By reversing the field direction of the solenoid (movie S3), the magnetic moment of the ferromagnetic liquid cylinder and the solenoid field are in antiparallel alignment and should repel each other. However, initially a slight attraction is seen because of the free MNPs in the cylinder core; then, the cylinder rotates, aligning the moment of the jammed MNP-surfactants with the solenoid field, and is drawn into the solenoid (Fig. 2B). Considering the low velocity (v_{max} ~1.1 × 10^{-4} m s^{-1}) and corresponding low Reynolds number (Re ~0.16), the velocity of the ferromagnetic liquid cylinders can be expressed approximately as a function of time: $v(t) = C\frac{ma}{b}(1 - e^{-bt/m})$, where C is a dimensionless constant based on Re and the shape of a liquid droplet, a is the acceleration from the drag force ($a = F_d / m$), m is the mass, and b is the coefficient of viscous friction. The constant velocity at longer times, independent of the initial magnetization configuration (Fig. 2B), implies a constant solenoid field gradient (due to the same M_s). Deviations from the linear relation in the early stage originate from viscous drag, the varying field gradient outside the solenoid, and the distinct initial magnetization configuration of the cylinder. Consequently, ferromagnetic liquid cylinders behave like solid magnets with N–N, S–S, and N–S dipole interactions. Figure 2C shows that magnetized liquid cylinders, initially separated by 1 mm, attract each other by such N–S dipole interactions (movie S4).

A distinguishing feature of the ferromagnetic liquid droplets is reconfigurability. A 3-μL spherical ferromagnetic liquid droplet (1.4-mm diameter) was drawn into a 1-mm-diameter glass capillary and then rapidly (after several seconds) ejected (Fig. 3, A and B, and movie S5). This transformed the spherical droplet into a cylinder (aspect ratio of 3:1). The interfacial area increased by 2.5 times, allowing more MNP-surfactants to form and jam, preserving the cylindrical shape. The ferromagnetic liquid droplet retained its ferromagnetic character, as evidenced by the rotation (~0.6 rad s^{-1}) in response to a rotating permanent magnetic field. The cylinder rotation is slightly less than that of the spherical droplet (~0.8 rad s^{-1}) because of the higher viscous drag force on the cylinder. The shape change can be reversed by tuning the binding energy, as shown in Fig. 3C, in which the pH was increased from 4.5 to 9, allowing the MNP-surfactants to unjam and the droplet shape to revert to spherical. Magnetization is lost, but by decreasing the pH, the MNP-surfactants rejam and the droplet transforms back to a ferromagnetic liquid droplet. Thus, the shape and magnetic state of the ferromagnetic liquid droplets are responsive.

The necessity of the magnetic coupling between the interfacially jammed MNP-surfactants and the dispersed MNPs to generate ferromagnetic liquid droplets is shown by changing the nature of the jammed interfacial assembly. Two sets of ferrofluid droplets at a pH of 4.5 were placed in a mixture of toluene and tetrachloride carbon of equal density containing POSS-NH_2 ligands: (i) ferrofluid droplets with carboxyl-functionalized 30-nm (22-nm core) Fe_3O_4 MNPs (0.5 g L^{-1}) that form ferromagnetic liquid droplets and (ii) a mixture of nonmagnetic sodium carboxymethyl cellulose (CMC-CO_2Na) (0.5 g L^{-1}) with 30-nm Fe_3O_4–polyethylene glycol (PEG) (nonfunctionalized) MNPs (0.5 g L^{-1}), in which only the CMC interacts with the POSS-NH_2. In both, nanoparticles jam at the interface (Fig. 4A), but in the first case they are ferromagnetic, whereas in the latter they are not ferromagnetic. Ferrofluid droplets of only PEG-functionalized Fe_3O_4 MNPs (0.5 g L^{-1}) were also placed in the oil. The total number of MNPs in all the droplets was constant. A bar magnet attracts all droplets (Fig. 4A) because all droplets have a ferromagnetic core, but the ferromagnetic liquid droplets are attracted much more strongly (Fig. 4A and movie S6). As shown in Fig. 4B, using a rotating magnet, the spherical ferromagnetic liquids rotate, whereas the unjammed ferrofluid and CMC-jammed ferrofluid droplets do not. The ferromagnetic liquid droplets are also attracted to the center of the magnet, and a dynamically stable pattern forms, balancing a hydrodynamic repulsion against a magnetic attraction, similar to that observed for elastomer discs (*15*, *16*) or ferrofluids (*17*, *18*) containing MNPs. Similar behavior is seen with ferromagnetic liquid cylinders in which the vortex flow in the oil is visualized with an oil-soluble dye (Fig. 4C and movie S7). The separation distance between the ferromagnetic liquid droplets depends on the rotation velocity (fig. S5 and movie S8), as expected. The entire patterned assembly of droplets also rotates in response to the rotating field. Upon stopping the rotating magnet, the ferromagnetic liquid cylinders align along the external field direction (movie S9). Absent of a dipole moment, the droplets with and without the jammed CMC monolayer do not spin and move only in a Brownian manner (movie S10). Therefore, the ferromagnetic liquid droplets can be easily separated, rotated in a controlled manner, and patterned (shown in Fig. 4B), affording a simple strategy for sorting and spatially arranging the ferromagnetic liquid droplets.

In conclusion, we have demonstrated the transformation of a ferrofluid to a ferromagnetic liquid droplet by the interfacial jamming and magnetization of MNP-surfactants. Ferromagnetic liquid droplets have the fluid characteristics of liquids but the magnetic properties of solids. They can be reconfigured while preserving their magnetic properties, and the attractive/repulsive interactions between ferromagnetic liquid droplets can be manipulated. Separation and patterning of ferromagnetic liquid droplets are easily achieved. The formation of ferromagnetic liquid droplets is reversible, and the interfacial assembly of the MNP-surfactants is responsive to external stimuli and provides systems in which translational and rotational motions can be actuated remotely and precisely by an external magnetic field.

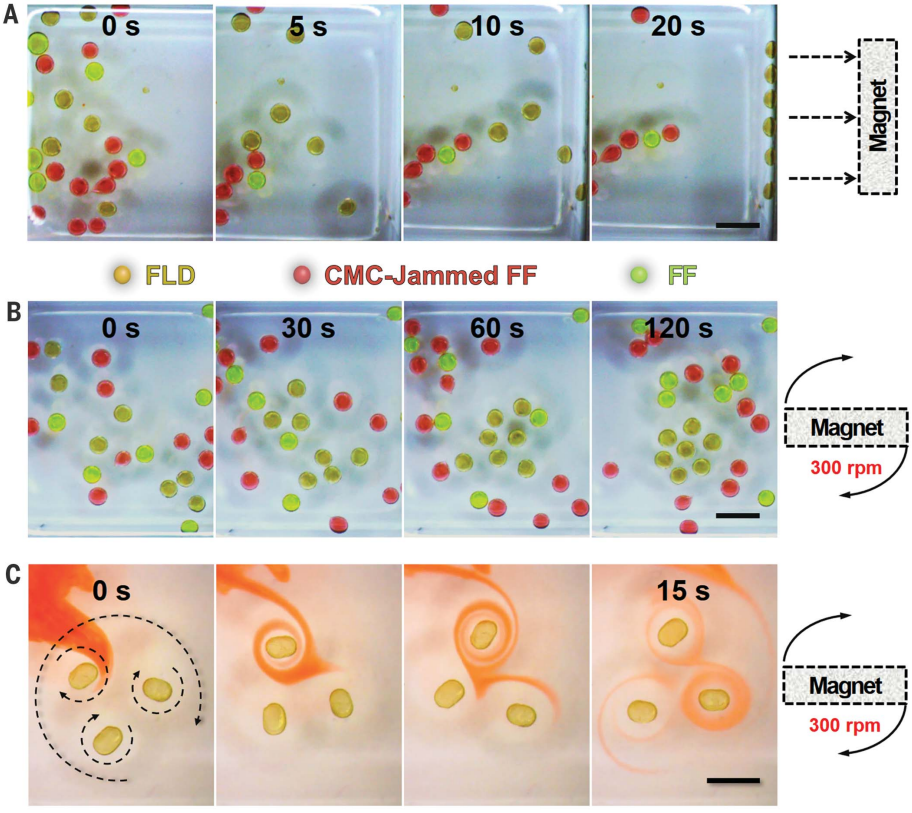

Fig. 4. Sorting FLDs by using static and rotational magnetic fields. Mixtures of FLDs comprising a shell of a jammed monolayer of MNP-surfactants and an FF core (dispersed carboxyl-functionalized iron oxide NPs, Fe_3O_4-CO_2H) (brownish spheres); FF droplet comprising a shell of jammed, nonmagnetic CMC surfactants (CMCSs) encapsulating an aqueous dispersion of PEG-coated iron oxide NPs (Fe_3O_4-PEG) (red spheres); FF droplet comprising an aqueous dispersion of Fe_3O_4-PEG NPs with no jammed monolayer at the droplet surface (bright green spheres). The separation of FLDs by using (**A**) a static bar magnet on the side of the container and (**B**) a bar magnet rotating under the container. [Rhodamine B in CMC-jammed FF] = 1 g L^{-1}, [fluorescein sodium salt in FF] = 1 g L^{-1}. (**C**) Visualization of the hydrodynamic vortex flow for an FLD ensemble in a rotating magnetic field using an oil-soluble dye. [Nile red in toluene] = 1 g L^{-1}. Scale bars, 3 mm.

REFERENCES AND NOTES

1. S. Odenbach, *MRS Bull.* **38**, 921–924 (2013).
2. R. E. Rosensweig, "Magnetic fluids" in *Ferrohydrodynamics* (Courier Corporation, 2013), pp. 34–44.
3. M. Cui, T. Emrick, T. P. Russell, *Science* **342**, 460–463 (2013).
4. Z. Zhang *et al.*, *Sci. Adv.* **4**, eaap8045 (2018).
5. A. H. Lu, E. L. Salabas, F. Schüth, *Angew. Chem. Int. Ed.* **46**, 1222–1244 (2007).
6. J. J. Benkoski *et al.*, *J. Am. Chem. Soc.* **129**, 6291–6297 (2007).
7. R. Streubel *et al.*, *Nano Lett.* **18**, 7428–7434 (2018).
8. E. C. Stoner, E. P. Wohlfarth, *Philos. Trans. R. Soc. London A* **240**, 599–642 (1948).
9. W. Luo, S. R. Nagel, T. F. Rosenbaum, R. E. Rosensweig, *Phys. Rev. Lett.* **67**, 2721–2724 (1991).
10. G. F. Goya, T. S. Berquó, F. C. Fonseca, M. P. Morales, *J. Appl. Phys.* **94**, 3520–3528 (2003).
11. X. Liu *et al.*, *Angew. Chem. Int. Ed.* **56**, 12594–12598 (2017).
12. J. Forth *et al.*, *Adv. Mater.* **30**, e1707603 (2018).
13. S. Shi *et al.*, *Adv. Mater.* **30**, 1705800 (2018).
14. A. Toor, S. Lamb, B. A. Helms, T. P. Russell, *ACS Nano* **12**, 2365–2372 (2018).
15. L. Derr, *Proc. Am. Acad. Arts Sci.* **44**, 525–528 (1909).
16. B. A. Grzybowski, H. A. Stone, G. M. Whitesides, *Nature* **405**, 1033–1036 (2000).
17. W. Wang, J. Giltinan, S. Zakharchenko, M. Sitti, *Sci. Adv.* **3**, e1602522 (2017).
18. J. V. I. Timonen, M. Latikka, L. Leibler, R. H. A. Ras, O. Ikkala, *Science* **341**, 253–257 (2013).

ACKNOWLEDGMENTS

Funding: This work was supported by the U.S. Department of Energy, Office of Science, Office of Basic Energy Sciences, Materials Sciences and Engineering Division (contract no. DE-AC02-05-CH11231) in the Adaptive Interfacial Assemblies Toward Structuring Liquids program (KCTR16). R.S., A.C., N.K., F.H, and P.F. acknowledge support from U.S. Department of Energy, Office of Science, Office of Basic Energy Sciences, Materials Sciences and Engineering Division (contract no. DE-AC02-05-CH11231) in the Non-equilibrium Magnetic Materials program (MSMAG). Work at the Molecular Foundry (AFM imaging) was supported by the Office of Science, Office of Basic Energy Sciences, of the U.S. Department of Energy (contract no. DE-AC02-05CH11231). S.S. was supported by the Beijing NSF (2194083). X.L. was supported by the Beijing Advanced Innovation Center for Soft Matter Science and Engineering at Beijing University of Chemical Technology and China Scholarship Council. **Author contributions:** X.L., N.K., R.S., B.A.H., P.D.A., P.F., and T.P.R. made contributions to the conception and design of the experiments. X.L., N.K., A.C., R.S., Y.J., Y.C., J.F., F.H., S.S., and D.W. performed and supported the experiments. X.L., N.K., R.S., P.Y.K., B.A.H., P.D.A., P.F., and T.P.R. interpreted the data and wrote the manuscript. **Competing interests:** P.D.A. is also associated with Scuba Probe Technologies. **Data and materials availability:** All data are available in the main text or the supplementary materials.

SUPPLEMENTARY MATERIALS

science.sciencemag.org/content/365/6450/264/suppl/DC1
Materials and Methods
Figs. S1 to S5
Table S1
Movies S1 to S10
References (*19*, *20*)

31 January 2019; accepted 24 May 2019
10.1126/science.aaw8719

Science

Reconfigurable ferromagnetic liquid droplets

Xubo Liu, Noah Kent, Alejandro Ceballos, Robert Streubel, Yufeng Jiang, Yu Chai, Paul Y. Kim, Joe Forth, Frances Hellman, Shaowei Shi, Dong Wang, Brett A. Helms, Paul D. Ashby, Peter Fischer and Thomas P. Russell

Science **365** (6450), 264-267.
DOI: 10.1126/science.aaw8719

Liquid reconfigurable ferromagnetic materials

Ferromagnetic materials show a permanent magnetic dipole, whereas superparamagnetic ones only show magnetic properties under an applied field. Some materials, like ferrofluids, show liquid-like behavior but do not retain their magnetization in the absence of an applied field. Liu *et al.* show remnant magnetization of otherwise superparamagnetic magnetite nanoparticles at an oil-water interface of emulsion droplets (see the Perspective by Dreyfus). The permanent magnetization could be controlled by coupling and uncoupling the magnetization of individual nanoparticles, making it possible to "write and erase" shapes of the droplets or to elongate them into cylinders.

Science, this issue p. 264; see also p. 219